

Stagnation and tearing of the subducting northwest Pacific slab

Muchen Sun¹, Youqiang Yu^{1*}, Stephen S. Gao² and Kelly H. Liu²¹State Key Laboratory of Marine Geology, Tongji University, Shanghai 200092, China²Geology and Geophysics Program, Missouri University of Science and Technology, Rolla, Missouri 65409, USA

ABSTRACT

Despite numerous observational and geodynamic modeling studies, the presence of the northwest Pacific slab tear and its influence on mantle dynamics remain controversial. By imaging the mantle transition zone (MTZ) discontinuities beneath the Japan Sea and adjacent areas, we demonstrate an ESE-WNW elongated zone with significant MTZ thinning extending from central Honshu, Japan, to the Korean Peninsula, which provides additional supporting evidence for the existence and distribution of a large-scale slab tear. Our results, when combined with other geophysical and geochemical evidence, indicate that the hot mantle material oceanward of the slab may flow through the slab tear and contribute to surface volcanism. Substantial MTZ thickening is widely observed in the region south of the slab tear and suggests the existence of slab stagnation, possibly related to the strong resistance at the bottom of the MTZ.

INTRODUCTION

The western Pacific plate is subducting beneath the Eurasian plate at a rate of ~ 9 cm/yr and beneath the Philippine Sea plate at ~ 6 cm/yr, resulting in the development of one of the largest trench-arc-backarc systems in the world (Fig. 1). This area is an ideal locale in which to investigate some critical issues associated with slab subduction, including the spatial distribution of the stagnant slab in the mantle transition zone (MTZ), the interaction of the subducting slab with the continental lithosphere, and the influence of slab subduction on the thermal structure of the upper mantle and MTZ (Obayashi et al., 2009; Zhao, 2021). Slab tearing of the subducting northwest Pacific plate has been proposed from a series of tomographic studies beneath different sites in the Japan Sea and adjacent areas, such as the Changbaishan volcano in northeastern China (Tang et al., 2014), central Honshu in Japan ($\sim 35^\circ\text{N}$; Obayashi et al., 2009), and the Izu-Bonin region ($\sim 28^\circ\text{N}$; Zhao et al., 2017), but the existence of a slab tear, spatial distribution, and their impacts on mantle dynamics remain debated. The controversy is mostly caused by the fact that a localized sharp reduction in the slab-related high-velocity anomalies determined from tomographic investigations is usually utilized to identify the slab tear (Obayashi et al., 2009). However, tomographic studies cannot

reliably distinguish between slab tearing and slab thinning solely on the basis of a reduction in the high-velocity anomalies, mostly due to the decreased resolution at greater depths and the effects of damping and smoothing regularization applied by most tomographic techniques. Thus, nontomographic geophysical investigations are necessary to further pinpoint the existence of slab tearing and corresponding geodynamic influences beneath the Japan Sea and its surrounding areas (Kennett and Furumura, 2010).

Geodynamic modeling studies (e.g., Facenna et al., 2010) suggest that focused mantle upwelling can be instigated near both the front and lateral edges of a subducting slab. One origin of subduction-related mantle upwelling could be the upward flux of mantle material caused by the displacement of a subducting slab, which can result in decompression melting as a result of buoyancy forces, which in turn can further promote additional upwelling (Facenna et al., 2010). Another proposed origin is the anomalously hot and buoyant asthenospheric material beneath the oceanic slab (Kawakatsu et al., 2009), which is dragged down by the subducting slab to the MTZ depth (Honda et al., 2007) and escapes through the slab tear or edges (Tang et al., 2014). However, the influence of subduction-induced mantle upwelling associated with the slab edges and tearing on the thermal structure of the MTZ remains unclear.

Seismological imaging of the topography of the MTZ discontinuities at 410 km (d410) and

660 km (d660) depth can provide independent constraints on the velocity and in situ temperature structure in the vicinity of the discontinuities (Shearer and Flanagan, 1999). The d410 represents the phase transition from olivine to spinel with a positive Clapeyron slope ranging from $+1.5$ MPa K^{-1} to $+4.0$ MPa K^{-1} , and the d660 is associated with the phase transition from ringwoodite to Mg perovskite + magnesio-wüstite with a negative Clapeyron slope ranging from -4.0 MPa K^{-1} to -0.2 MPa K^{-1} (Bina and Helffrich, 1994; Fei et al., 2004; Tauzin and Ricard, 2014). Given the opposite sign of the Clapeyron slopes for the d410 and d660, high and low thermal anomalies would lead to thinned and thickened MTZ, respectively, which helps to provide important information on the spatial distribution of the stagnant slab in the MTZ and mantle upwelling around MTZ discontinuities (Bina and Helffrich, 1994).

Several receiver function (RF) MTZ studies have been conducted in northeastern China (Ai et al., 2003; Li and Yuan, 2003; Liu et al., 2015; Zhang et al., 2016; Sun et al., 2020), and the general conclusion is that the subducting Pacific slab has reached the d660 within a narrow area based on a regionally thickened MTZ associated with a depressed d660. A narrow zone of uplifted d410 and a broad zone with depressed d660 were observed beneath southwestern Japan (Niu et al., 2005), indicating that the subducting slab is deflected when it reaches the MTZ boundaries, and it is flat-lying above or across the d660. Lee et al. (2014) found a depressed d410 extending from the Korean Peninsula to Kyushu Island and a N-S variation in the depth of the d660, with an obvious depression south of 36°N , which was explained by different angles of slab subduction. Additionally, they also observed a depressed d410 around the tip of the slab tear reported by Obayashi et al. (2009), when a one-dimensional (1-D) velocity model was utilized for time-depth conversion, but the feature became unclear when a three-dimensional (3-D) velocity model was used.

*E-mail: yuyouqiang@tongji.edu.cn

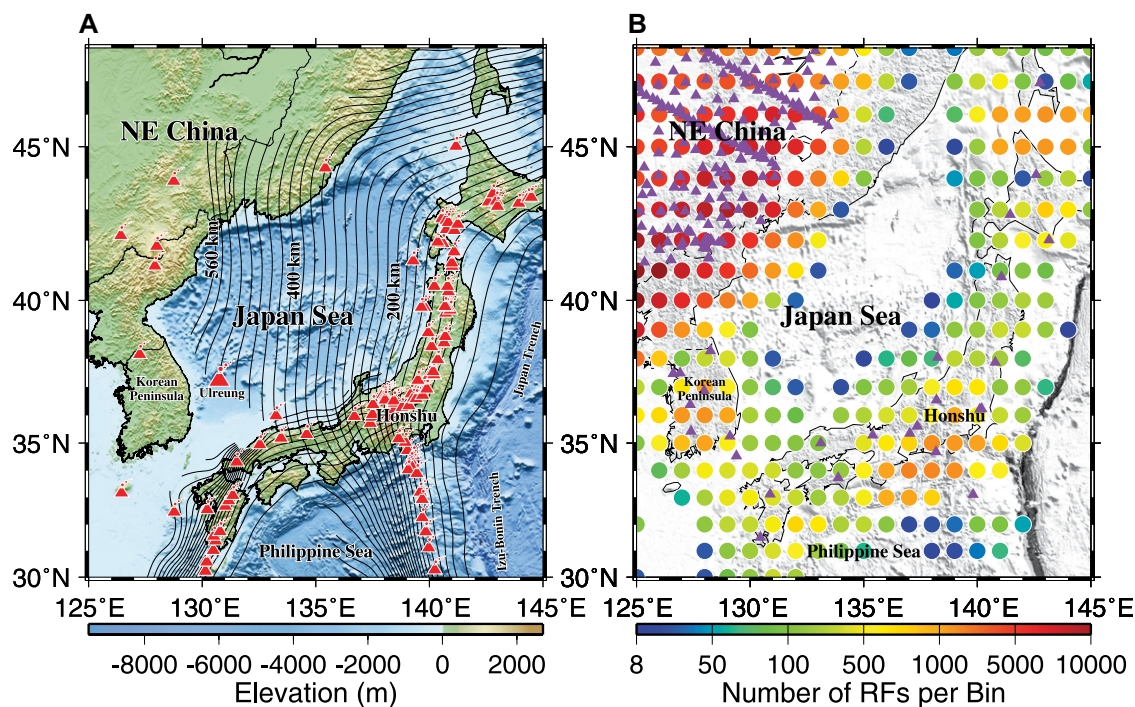


Figure 1. Tectonic setting and data used in this study. (A) Topographic map of the Japan Sea and adjacent areas showing Cenozoic volcanoes (red triangles) and contour depths of subducting slabs (black lines). (B) Distributions of seismic stations (purple triangles) and number of receiver functions (RFs, colored dots) for each bin with a radius of 1 degree at a depth of 535 km.

To provide additional constraints on several controversial issues related to the spatial distribution of the subducting slab in the vicinity of the MTZ and subduction-related mantle upwelling, large numbers (139,740) of P-to-S RFs were moveout-corrected and stacked using the IASP91 Earth model (Kennett and Engdahl, 1991) and the 3-D TX2019slab model (Lu et al., 2019) to produce robust images of the MTZ discontinuities beneath the Japan Sea and adjacent areas (see the Supplemental Material¹ for details on the data, methods, and individual measurements). We divided the study region into five subareas based on the patterns of the resulting MTZ discontinuity depths and thicknesses for further discussion (Fig. 2).

SLAB STAGNATION IN THE MTZ

An approximately north-south-oriented narrow zone (area A) adjacent to the western edge of the Pacific slab Wadati-Benioff zone in north-eastern China is characterized by significant MTZ thickening (~16–21 km; Table 1) with a large depression of the d660 (~30–31 km). Given the observation of the slab-related high-velocity anomalies over the MTZ bottom (Fig. S1A; Chen et al., 2017), the significant depression of the d660 and MTZ thickening imply that the subducting slab contacts closely with the

d660 beneath this area. Such a conclusion is consistent with previous MTZ studies in north-eastern China (Ai et al., 2003; Li and Yuan, 2003; Liu et al., 2015; Zhang et al., 2016; Sun et al., 2020). Area B is bounded by the 400 km and 560 km depth contour lines of the subducting Pacific slab (Fig. 2). The magnitude of the observed apparent MTZ thinning decreased significantly after velocity correction (Fig. 2F), indicating that the MTZ thinning beneath area B is mainly caused by a high-velocity anomaly associated with the subducting slab between the top and bottom of the MTZ (Sun et al., 2020), which has also been identified by a tomographic study (Fig. S1A; Chen et al., 2017). A previously proposed small-scale slab window associated with stagnation of the descending Pacific slab in this area (Zhang et al., 2016) may contribute to the residual ~10 km MTZ thinning after velocity correction beneath the central part of area B.

Significant MTZ thickening both before and after velocity correction (Table 1) is widely revealed beneath area C and mostly results from an enormously depressed d660 (684 ± 12 km) with a normal d410 (409 ± 9 km). Similar observation of a thickened MTZ was also reported from previous RF studies around this area (Niu et al., 2005; Lee et al., 2014; Wang et al., 2017; Tauzin et al., 2018) and was interpreted as a result of a narrow uplift of the d410 and a broad depression of the d660. Assuming a scaling factor of $dV_p/dT = 4.8 \times 10^{-4} \text{ km s}^{-1} \text{ K}^{-1}$ and a Clapeyron slope of -1.3 MPa K^{-1} for the d660 (Fei et al., 2004), the observed 24 km depression of the d660 corresponds to an ~670 K temperature decrease relative to the surrounding mantle. Such a thermal anomaly is

generally consistent with the temperature difference of 700 K between the surrounding mantle and the coldest core of the slab at the bottom of the MTZ (Kawakatsu and Yoshioka, 2011). The significantly depressed d660 and the normal d410 combined with high-velocity anomalies in the MTZ from previous tomography studies (Fig. S1B) suggest that the substantial MTZ thickening beneath area C is most likely induced by a direct thermal effect associated with the stagnant slab at the bottom of the MTZ. The slab stagnation can be explained by the strong resistance from buoyancy effects caused by the mineral phase change from spinel to postspinel and viscosity jump at the d660 (Chen et al., 2017; Ma et al., 2019). A stagnant and flat slab has also been imaged north of 28°N beneath the Izu-Bonin region (Zhao et al., 2017).

EXISTENCE AND IMPACTS OF A SLAB TEAR

An east-southeast–west-northwest elongated zone (area D) with 10–15 km of thinning of the MTZ (Table 1) is revealed to extend from southwest Japan to the Korean Peninsula, sandwiched between MTZ thickening areas A and C (Fig. 2). The close-to-normal depths of the d660 before and after velocity correction (Fig. 2; Table 1) may rule out the thermal effect from a subducted slab at the bottom of the MTZ. Instead, the thinner-than-normal MTZ thickness and depressed d410 may suggest the existence of a high thermal anomaly traversing the d410, which is possibly associated with slab tearing (Fig. 3).

A vertical slab tear of the westward-subducting Pacific slab (Fig. 3) has occurred beneath central Honshu, Japan, which is evidenced

¹Supplemental Material. Figure S1 (stacked receiver functions along 34°N, 35°N, 36°N, and 43°N latitudinal lines), and Table S1 (results of receiver function stacking for each bin). Please visit <https://doi.org/10.1130/GEOL.S.19176242> to access the supplemental material, and contact editing@geosociety.org with any questions.

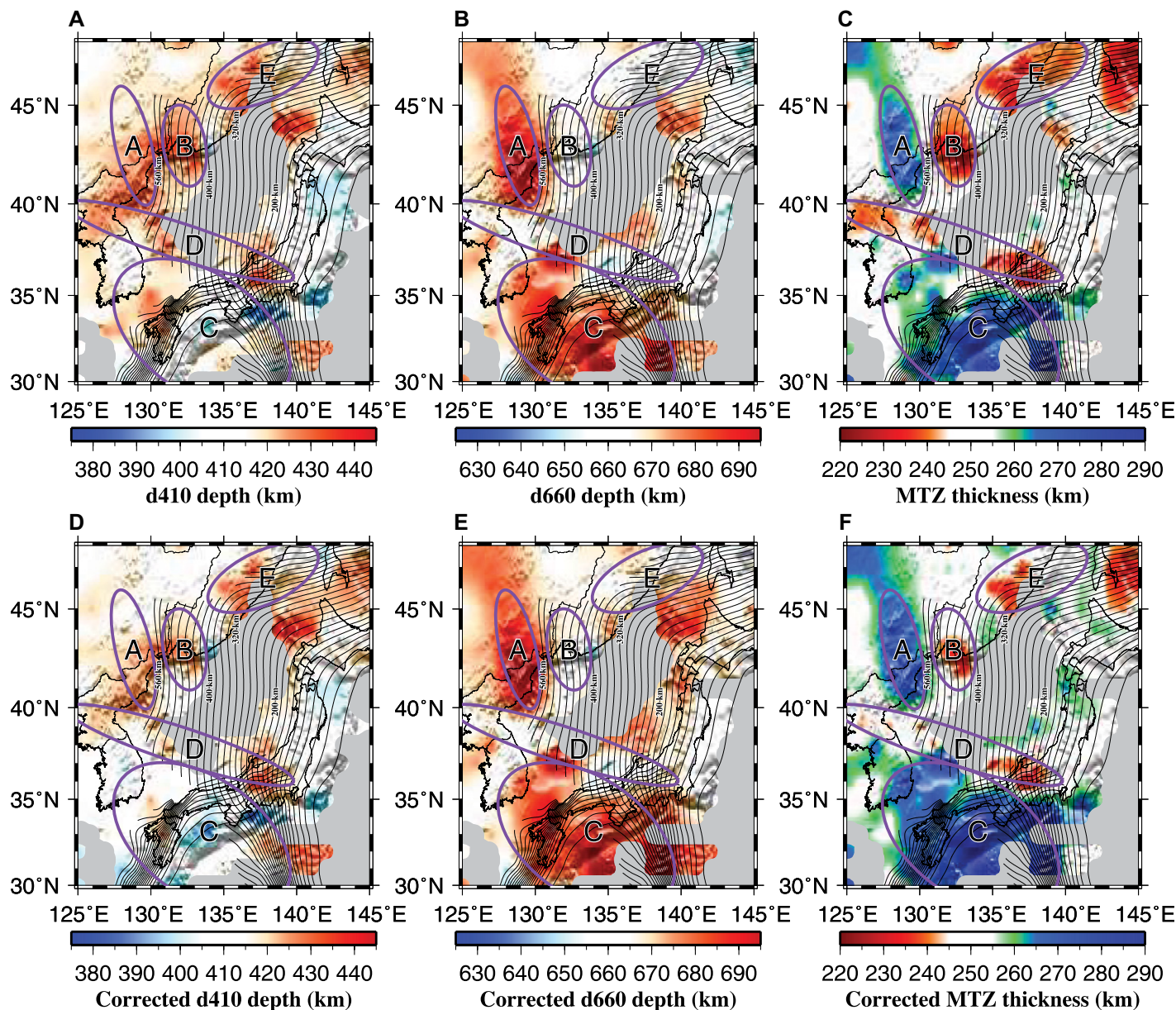


Figure 2. Resulting mantle transition zone (MTZ) discontinuity depths and thickness. (A–C) Spatial distributions of resulting apparent depths of the 410 km and 660 km discontinuities (d410 and d660, respectively), and MTZ thickness measurements. (D–F) Same as A–C but after the velocity correction from the TX2019slab model (Lu et al., 2019). Ellipses mark five subareas (areas A–E) discussed in the text.

by the absence of the subduction-related high-velocity anomalies in the tearing region, the occurrence of lateral tension-type earthquakes near the slab tear tip, and the observation of a close-to-vertical plane related to a side-wall of the slab tear (Obayashi et al., 2009). The combined effect of several factors is believed

to result in the slab tearing, including the variable subduction angle, rate, and dip between the two slab segments (Ma et al., 2019), and the bending and flattening of the subducting slab atop the d660 (Fig. 3; Obayashi et al., 2009). The slab tear propagated from the tip (~35°N, 138°E) beneath southwest Japan westward to the

Korean Peninsula (Obayashi et al., 2009, their figures 2 and 3), which generally matches with the observed MTZ thinning in area D (Fig. 2). This coincidence provides additional supporting evidence for the existence of a large-scale slab tear and further confirms its range. Assuming a Clapeyron slope of +2.9 MPa K⁻¹ for the

TABLE 1. MEAN MEASUREMENTS FOR THE FIVE SUBAREAS IN THE JAPAN SEA AND ADJACENT AREAS BEFORE AND AFTER VELOCITY CORRECTION

Area	d410 (IASP91) (km)	d660 (IASP91) (km)	MTZ (IASP91) (km)	d410 (TX2109) (km)	d660 (TX2019) (km)	MTZ (TX2019) (km)
Entire study area	417 ± 10	670 ± 13	252 ± 14	415 ± 10	673 ± 13	258 ± 15
A	424 ± 6	690 ± 10	266 ± 7	420 ± 5	691 ± 9	271 ± 7
B	427 ± 8	665 ± 5	238 ± 9	421 ± 8	665 ± 5	244 ± 9
C	414 ± 10	682 ± 11	268 ± 13	409 ± 9	684 ± 12	275 ± 14
D	426 ± 8	661 ± 6	235 ± 9	423 ± 9	663 ± 6	240 ± 10
E	423 ± 10	660 ± 4	236 ± 8	421 ± 10	663 ± 3	242 ± 9

Note: d410 and d660—410 km and 660 km discontinuities; MTZ—mantle transition zone; IASP91 and TX2019—Earth velocity models.

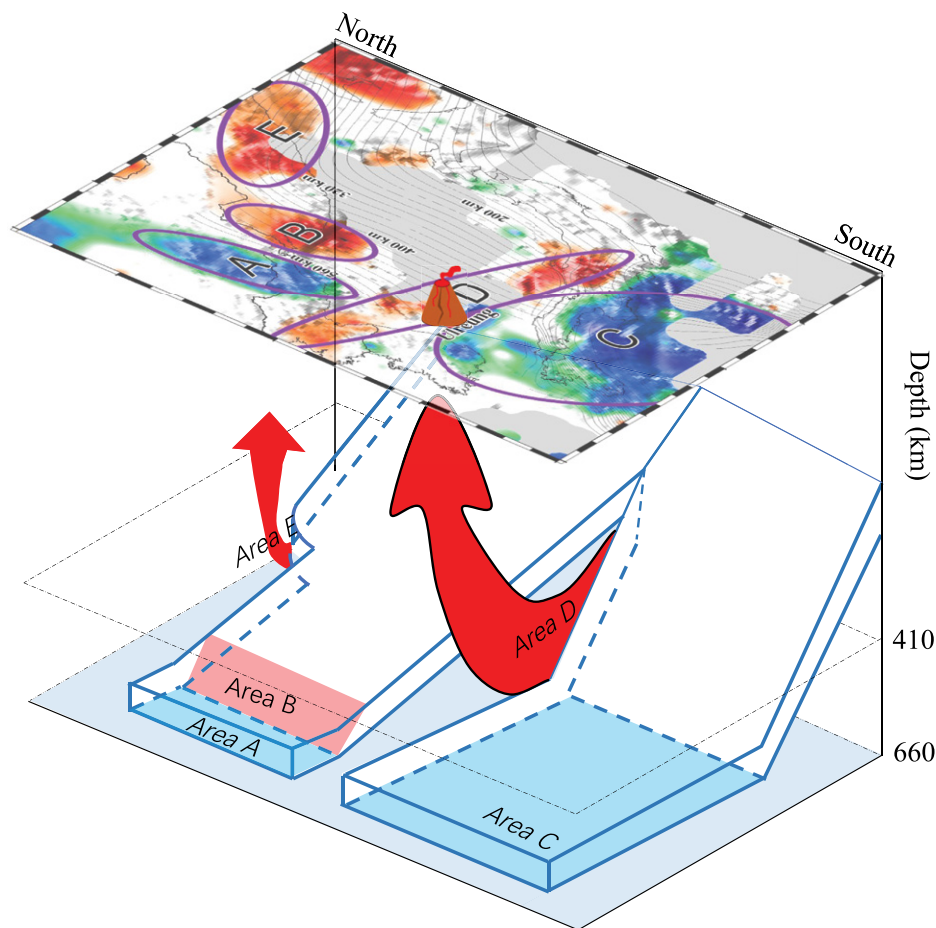


Figure 3. Schematic sketch of the subducting northwest Pacific slab beneath the study area. Blue and red marked zones represent subareas with observed mantle transition zone (MTZ) thickening and thinning, respectively. Red arrows represent mantle flow around slab edges or slab tearing. Volcano icon on the map represents the Ulreung volcano.

d410 (Bina and Helffrich, 1994), the observed ~ 13 km depression of the d410 corresponds to an ~ 160 K high-temperature anomaly around the top of the MTZ beneath area D. Such a temperature anomaly is generally consistent with the reported 150 K high-temperature anomaly at 350 km depth oceanward of the Honshu slab (Obayashi et al., 2006; Bagley et al., 2009), which is possibly caused by the long-term trench rollback of the Pacific slab (Wang et al., 2017). A recent 3-D P-wave anisotropy study (Ma et al., 2019) observed a striking counter-clockwise rotation of the fast-velocity direction around the slab tear. Such a pattern can be attributed to the complex mantle flow system passing through the slab tear due to the great difference in the pressure gradient between the mantle wedge above the Pacific plate and the subplate mantle (Ma et al., 2019). The hot and buoyant mantle upwelling flow through the slab tear can melt the subducting slab, leading to the formation of mafic magmas, such as those associated with adakites in southwest Japan (Nguyen et al., 2020). In addition, the isotopic components of the basalts on the surface above the slab tear are characterized by higher $^{208}\text{Pb}/^{204}\text{Pb}$ but lower

$^{207}\text{Pb}/^{204}\text{Pb}$, which are considered to result from the detachment of buoyant seamount portions from the subducting plate during slab break-off, when it reached the MTZ, and subsequent incorporation into the mantle upwelling flow (Nguyen et al., 2020). Therefore, when combined the above geophysical and geochemical observations, we propose that the hot mantle material may flow through the slab tear and rise across the d410 (Fig. 3), leading to surface volcanic activities along the slab tearing zone, such as at Ulreung volcano.

The Ulreung volcano, a Holocene intraplate volcano, is located above the southern edge of the observed slab tear beneath area D (Fig. 1) and underlain by thinned continental crust (Kim et al., 2011). A recent petrogenesis study (Choi, 2021) revealed that the Ulreung basalts might have been derived from a hydrous-phase-bearing, hybrid pyroxenite-garnet-peridotite source at the MTZ depth. Wei and Zhao (2020) found a clear low-velocity anomaly down to ~ 400 km in the upper mantle and deemed that the deep subduction and dehydration of the subducted Pacific slab may contribute to the Ulreung intraplate volcanism. Given that the low-velocity

anomaly beneath the Ulreung volcano seems to go down eastward and connect to the slab tearing or thinning zone identified by an obvious reduction in the high-velocity anomaly (Wei and Zhao, 2020), we propose an alternative model in which the slab tear beneath area D may act as a channel where anomalously hot, buoyant mantle material can rise, consequently inducing decompression melting in the upper mantle, which feeds the intraplate Ulreung volcano. Similarly, Tang et al. (2014) observed a Pacific slab tear beneath northeastern China and attributed the Changbaishan basaltic magmatism to slab subduction-induced warm material upwelling through a slab tear.

MANTLE UPWELLING NEAR SLAB EDGES

Besides slab tearing, a depressed d410 and significant MTZ thinning are observed around the northern edge of the Pacific slab (area E), in the area extending approximately from the 320 km depth contour line of the subducting slab to the edge of the detectable Wadati-Benioff zone. The 11–13 km depression of the d410 corresponds to an ~ 130 – 160 K temperature increase around the d410, which is also comparable to the high-temperature anomaly oceanward of the Honshu slab (Obayashi et al., 2006; Bagley et al., 2009). Combining the presence of low-velocity anomalies in the upper mantle and upper MTZ (Lu et al., 2019), our results suggest that subslab hot material may flow around the slab edge, leading to a zone with high-temperature anomalies and thinned MTZ (Fig. 3). Such mantle flow around slab edges has also been observed in several worldwide sites, such as the southern half of the Kamchatka Peninsula (Levin et al., 2002; Jiang et al., 2009) and eastern Alaska (Dahm et al., 2017).

CONCLUSIONS

In this study, we systematically explored the MTZ structure beneath the Japan Sea and adjacent areas. The main conclusions include the following: (1) An east-southeast–west-northwest elongated region with significant MTZ thinning extending from central Honshu, Japan, to the Korean Peninsula, which is characterized by a depressed d410 and normal d660, may be attributed to mantle flow through a slab tear. (2) The area around the northern edge of the Pacific slab is also characterized by significant thinning of the MTZ, indicating the existence of thermal mantle flow at the slab edge. (3) MTZ thickening is widely observed beneath the southwestern Japan portion of the northern Philippine Sea, and it possibly indicates the existence of a stagnant slab atop the d660.

ACKNOWLEDGMENTS

We appreciate the Data Management Centers of the Incorporated Research Institutions for Seismology

(IRIS; <https://ds.iris.edu/ds/nodes/dmc/>) and the Data Management Centre of the China National Seismic Network at the Institute of Geophysics, China Earthquake Administration (SEISDMC; <http://www.seisdmc.ac.cn>), for providing teleseismic data used in this study. Constructive comments from editor Urs Schaltegger and two anonymous reviewers significantly improved the manuscript. The study was supported by the National Natural Science Foundation of China (grants 42006058 and 42074052) and the China Postdoctoral Science Foundation (grant 2019M661607).

REFERENCES CITED

- Ai, Y., Zheng, T., Xu, W., He, Y., and Dong, D., 2003, A complex 660 km discontinuity beneath northeast China: *Earth and Planetary Science Letters*, v. 212, p. 63–71, [https://doi.org/10.1016/S0012-821X\(03\)00266-8](https://doi.org/10.1016/S0012-821X(03)00266-8).
- Bagley, B., Courtier, A.M., and Revenaugh, J., 2009, Melting in the deep upper mantle oceanward of the Honshu slab: *Physics of the Earth and Planetary Interiors*, v. 175, p. 137–144, <https://doi.org/10.1016/j.pepi.2009.03.007>.
- Bina, C.R., and Helffrich, G., 1994, Phase transition Clapeyron slopes and transition zone seismic discontinuity topography: *Journal of Geophysical Research: Solid Earth*, v. 99, p. 15853–15860, <https://doi.org/10.1029/94JB00462>.
- Chen, C., Zhao, D., Tian, Y., Wu, S., Hasegawa, A., Lei, J., Park, J.H., and Kang, I.B., 2017, Mantle transition zone, stagnant slab and intraplate volcanism in northeast Asia: *Geophysical Journal International*, v. 209, p. 68–85, <https://doi.org/10.1093/gji/ggw491>.
- Choi, S.H., 2021, Geochemistry and petrogenesis of Quaternary volcanic rocks from Ulleung Island, South Korea: *Lithos*, v. 380–381, p. 105874, <https://doi.org/10.1016/j.lithos.2020.105874>.
- Dahm, H.H., Gao, S.S., Kong, F., and Liu, K.H., 2017, Topography of the mantle transition zone discontinuities beneath Alaska and its geodynamic implications: Constraints from receiver function stacking: *Journal of Geophysical Research: Solid Earth*, v. 122, p. 10352–10363, <https://doi.org/10.1002/2017JB014604>.
- Faccenna, C., Becker, T.W., Lallemand, S., Lagabriele, F., Funicello, F., and Piromallo, C., 2010, Subduction-triggered magmatic pulses: A new class of plumes?: *Earth and Planetary Science Letters*, v. 299, p. 54–68, <https://doi.org/10.1016/j.epsl.2010.08.012>.
- Fei, Y., Van Orman, J., Li, J., Van Westrenen, W., Sanloup, C., Minarik, W., Hirose, K., Komabayashi, T., Walter, M., and Funakoshi, K.I., 2004, Experimentally determined postspinel transformation boundary in Mg_2SiO_4 using MgO as an internal pressure standard and its geophysical implications: *Journal of Geophysical Research: Solid Earth*, v. 109, B02305, <https://doi.org/10.1029/2003JB002562>.
- Honda, S., Morishige, M., and Orihashi, Y., 2007, Sinking hot anomaly trapped at the 410 km discontinuity near the Honshu subduction zone, Japan: *Earth and Planetary Science Letters*, v. 261, p. 565–577, <https://doi.org/10.1016/j.epsl.2007.07.028>.
- Jiang, G., Zhao, D., and Zhang, G., 2009, Seismic tomography of the Pacific slab edge under Kamchatka: *Tectonophysics*, v. 465, p. 190–203, <https://doi.org/10.1016/j.tecto.2008.11.019>.
- Kawakatsu, H., and Yoshioka, S., 2011, Metastable olivine wedge and deep dry cold slab beneath southwest Japan: *Earth and Planetary Science Letters*, v. 303, p. 1–10, <https://doi.org/10.1016/j.epsl.2011.01.008>.
- Kawakatsu, H., Kumar, P., Takei, Y., Shinohara, M., Kanazawa, T., Araki, E., and Suyehiro, K., 2009, Seismic evidence for sharp lithosphere-asthenosphere boundaries of oceanic plates: *Science*, v. 324, p. 499–502, <https://doi.org/10.1126/science.1169499>.
- Kennett, B.L.N., and Engdahl, E.R., 1991, Traveltimes for global earthquake location and phase identification: *Geophysical Journal International*, v. 105, p. 429–465, <https://doi.org/10.1111/j.1365-246X.1991.tb06724.x>.
- Kennett, B.L.N., and Furumura, T., 2010, Tears or thinning? Subduction structures in the Pacific plate beneath the Japanese Islands: *Physics of the Earth and Planetary Interiors*, v. 180, p. 52–58, <https://doi.org/10.1016/j.pepi.2010.03.001>.
- Kim, G.B., Yoon, S.H., Chough, S.K., Kwon, Y.K., and Ryu, B.J., 2011, Seismic reflection study of acoustic basement in the South Korea Plateau, the Ulleung Interplain Gap, and the northern Ulleung Basin: Volcano-tectonic implications for Tertiary back-arc evolution in the southern East Sea: *Tectonophysics*, v. 504, p. 43–56, <https://doi.org/10.1016/j.tecto.2011.02.004>.
- Lee, S.H., Rhie, J., Park, Y., and Kim, K.H., 2014, Topography of the 410 and 660 km discontinuities beneath the Korean Peninsula and southwestern Japan using teleseismic receiver functions: *Journal of Geophysical Research: Solid Earth*, v. 119, p. 7245–7257, <https://doi.org/10.1002/2014JB011149>.
- Levin, V., Shapiro, N., Park, J., and Ritzwoller, M., 2002, Seismic evidence for catastrophic slab loss beneath Kamchatka: *Nature*, v. 418, p. 763–767, <https://doi.org/10.1038/nature00973>.
- Li, X., and Yuan, X., 2003, Receiver functions in northeast China—Implications for slab penetration into the lower mantle in northwest Pacific subduction zone: *Earth and Planetary Science Letters*, v. 216, p. 679–691, [https://doi.org/10.1016/S0012-821X\(03\)00555-7](https://doi.org/10.1016/S0012-821X(03)00555-7).
- Liu, Z., Niu, F., Chen, Y.J., Grand, S., Kawakatsu, H., Ning, J., Tanaka, S., Obayashi, M., and Ni, J., 2015, Receiver function images of the mantle transition zone beneath NE China: New constraints on intraplate volcanism, deep subduction and their potential link: *Earth and Planetary Science Letters*, v. 412, p. 101–111, <https://doi.org/10.1016/j.epsl.2014.12.019>.
- Lu, C., Grand, S.P., Lai, H., and Garnero, E.J., 2019, TX2019slab: A new P and S tomography model incorporating subducting slabs: *Journal of Geophysical Research: Solid Earth*, v. 124, p. 11549–11567, <https://doi.org/10.1029/2019JB017448>.
- Ma, J., Tian, Y., Zhao, D., Liu, C., and Liu, T., 2019, Mantle dynamics of western Pacific and East Asia: New insights from P wave anisotropic tomography: *Geochemistry Geophysics Geosystems*, v. 20, p. 3628–3658, <https://doi.org/10.1029/2019GC008373>.
- Nguyen, T.T., Kitagawa, H., Pineda-Velasco, I., and Nakamura, E., 2020, Feedback of slab distortion on volcanic arc evolution: Geochemical perspective from late Cenozoic volcanism in SW Japan: *Journal of Geophysical Research: Solid Earth*, v. 125, e2019JB019143, <https://doi.org/10.1029/2019JB019143>.
- Niu, F., Levander, A., Ham, S., and Obayashi, M., 2005, Mapping the subducting Pacific slab beneath southwest Japan with Hi-net receiver functions: *Earth and Planetary Science Letters*, v. 239, p. 9–17, <https://doi.org/10.1016/j.epsl.2005.08.009>.
- Obayashi, M., Sugioka, H., Yoshimitsu, J., and Fukao, Y., 2006, High temperature anomalies oceanward of subducting slabs at the 410-km discontinuity: *Earth and Planetary Science Letters*, v. 243, p. 149–158, <https://doi.org/10.1016/j.epsl.2005.12.032>.
- Obayashi, M., Yoshimitsu, J., and Fukao, Y., 2009, Tearing of stagnant slab: *Science*, v. 324, p. 1173–1175, <https://doi.org/10.1126/science.1172496>.
- Shearer, P.M., and Flanagan, M.P., 1999, Seismic velocity and density jumps across the 410- and 660-kilometer discontinuities: *Science*, v. 285, p. 1545–1548, <https://doi.org/10.1126/science.285.5433.1545>.
- Sun, M., Gao, S.S., Liu, K.H., and Fu, X., 2020, Upper mantle and mantle transition zone thermal and water content anomalies beneath NE Asia: Constraints from receiver function imaging of the 410 and 660 km discontinuities: *Earth and Planetary Science Letters*, v. 532, 116040, <https://doi.org/10.1016/j.epsl.2019.116040>.
- Tang, Y., Obayashi, M., Niu, F., Grand, S.P., Chen, Y.J., Kawakatsu, H., Tanaka, S., Ning, J., and Ni, J.F., 2014, Changbaishan volcanism in northeast China linked to subduction-induced mantle upwelling: *Nature Geoscience*, v. 7, p. 470–475, <https://doi.org/10.1038/ngeo2166>.
- Tauzin, B., and Ricard, Y., 2014, Seismically deduced thermodynamics phase diagrams for the mantle transition zone: *Earth and Planetary Science Letters*, v. 401, p. 337–346, <https://doi.org/10.1016/j.epsl.2014.05.039>.
- Tauzin, B., Kim, S., and Afonso, J.C., 2018, Multiple phase changes in the mantle transition zone beneath northeast Asia: Constraints from teleseismic reflected and converted body waves: *Journal of Geophysical Research: Solid Earth*, v. 123, p. 6636–6657, <https://doi.org/10.1029/2017JB015238>.
- Wang, X., Li, J., and Chen, Q.F., 2017, Topography of the 410 km and 660 km discontinuities beneath the Japan Sea and adjacent regions by analysis of multiple-ScS waves: *Journal of Geophysical Research: Solid Earth*, v. 122, p. 1264–1283, <https://doi.org/10.1002/2016JB013357>.
- Wei, W., and Zhao, D., 2020, Intraplate volcanism and mantle dynamics of Mainland China: New constraints from shear-wave tomography: *Journal of Asian Earth Sciences*, v. 188, p. 104103, <https://doi.org/10.1016/j.jseas.2019.104103>.
- Zhang, R., Gao, Z., Wu, Q., Xie, Z., and Zhang, G., 2016, Seismic images of the mantle transition zone beneath northeast China and the Sino-Korean craton from P-wave receiver functions: *Tectonophysics*, v. 675, p. 159–167, <https://doi.org/10.1016/j.tecto.2016.03.002>.
- Zhao, D., 2021, Seismic imaging of northwest Pacific and East Asia: New insight into volcanism, seismogenesis and geodynamics: *Earth-Science Reviews*, v. 214, 103507, <https://doi.org/10.1016/j.earscirev.2021.103507>.
- Zhao, D., Fujisawa, M., and Toyokuni, G., 2017, Tomography of the subducting Pacific slab and the 2015 Bonin deepest earthquake (Mw 7.9): *Scientific Reports*, v. 7, 44487, <https://doi.org/10.1038/srep44487>.

Printed in USA